LASER INTERFEROMETER GRAVITATIONAL WAVE OBSERVATORY
- LIGO -
CALIFORNIA INSTITUTE OF TECHNOLOGY
MASSACHUSETTS INSTITUTE OF TECHNOLOGY

Technical Note **LIGO-T1500228-v1** 2015/06/03

Progress report 1: Sensing and control of suspended optic breadboard in Crackle2 experiment

Sai Kanth Dacha | Mentors: Gabriele Vajente, Rana Adhikari

Distribution of this document:

LIGO Scientific Collaboration

California Institute of Technology
LIGO Project, MS 18-34
Pasadena, CA 91125
Phone (626) 395-2129
Fax (626) 304-9834
E-mail: info@ligo.caltech.edu

Massachusetts Institute of Technology
LIGO Project, Room NW17-161
Cambridge, MA 02139
Phone (617) 253-4824
Fax (617) 253-7014
E-mail: info@ligo.mit.edu

LIGO Hanford Observatory
Route 10, Mile Marker 2
Richland, WA 99352
Phone (509) 372-8106
Fax (509) 372-8137
E-mail: info@ligo.caltech.edu

LIGO Livingston Observatory
19100 LIGO Lane
Livingston, LA 70754
Phone (225) 686-3100
Fax (225) 686-7189
E-mail: info@ligo.caltech.edu

http://www.ligo.caltech.edu/

1 Introduction

In metals, dislocations are 'pinned' by obstacles like grain boundaries or other surfaces. (Dislocations are dis-junctions in the periodic lattice structure.) Under small oscillatory stress, these dislocation lines bow in and out, but the response of the complex network on the whole is known to act nonlinearly through long-range interactions between dislocations. This nonlinear behavior, among a broad class of other nonlinear phenomena, is known to be the cause of "crackling". "Crackling" here refers to impulsive releases of energy, acoustic emissions, or changes in the geometry of attachments between suspension elements. It has been suspected that this "crackling noise" in various components and suspensions might produce excess noise in aLIGO. [1]

Many possible locations of crackle have been identified, some of which are:

- The maraging steel blades used for vertical isolation
- The silica fibers which suspend the test masses from the penultimate masses
- The welds which attach the fibers to the ears
- The clamps which hold the suspension wires to the steel blades

Figure 1 shows the test mass suspension scheme in Advanced LIGO.

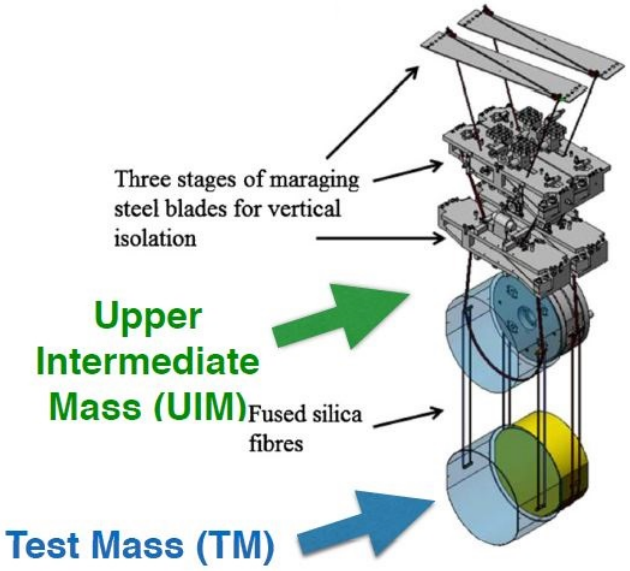

Figure 1: Suspension scheme in Advanced LIGO

The maraging steel blades have been under investigation in the first crackle experiments, as they present a mechanical system which can be driven and stressed easily. In addition, mechanical

crackling noise is sufficiently generic that an experiment capable of measuring this noise in maraging steel blade springs will be well suited for investigating crackling in other components used in aLIGO as well.

As crackling noise is inherently nonlinear, there is the potential for noise to be upconverted. Specifically, motion of the suspension at sub-Hz microseismic frequencies may induce blade motion, causing the blades internal stresses to fluctuate, resulting in an avalanche of crackle events with high-frequency content. As we do not currently possess a reliable analytical model to predict the magnitude, or frequency dependence, of the these events, we hope to do so experimentally directly at the frequencies of interest. [1]

2 Where I started

This section describes the work that was already done before my arrival. I picked up one part of the Crackle2 experiment - suspension damping of the breadboard - and I started off in direction of establishing a feedback damping control loop for it.

2.1 Measurement strategy

With reference to figure 1, below the upper intermediate mass (UIM) in the quadruple suspension system, there is no more spring blade isolation, thus any crackling noise in the UIM maraging steel blades will propagate directly to the test mass. Therefore, one would want to ensure low enough crackling noise at the UIM blade tip itself.

A direct measurement of crackling noise is very difficult. However, one can make measurements of the blade displacements directly using a Michelson interferometer with end mirrors mounted to loaded blade springs which are driven with a low frequency, common-mode force. Since crackling noise occurs incoherently in each blade, it will show up in the Michelson's displacement signal. In order to ensure repeatability and applicability of results, the setup has been made to be similar to the existing aLIGO configuration.

2.2 Experimental design

The setup consists of a Michelson interferometer using blade-suspended masses as end mirrors. A crackle event will change the differential displacement of the mirrors, and hence be reflected in the interferometer output. The events are excited by a low frequency, common-mode, drive on the two blades. [1] The apparatus is going to be housed in a vacuum chamber to mitigate acoustic noise.

Figure 2 is a picture of the full setup.

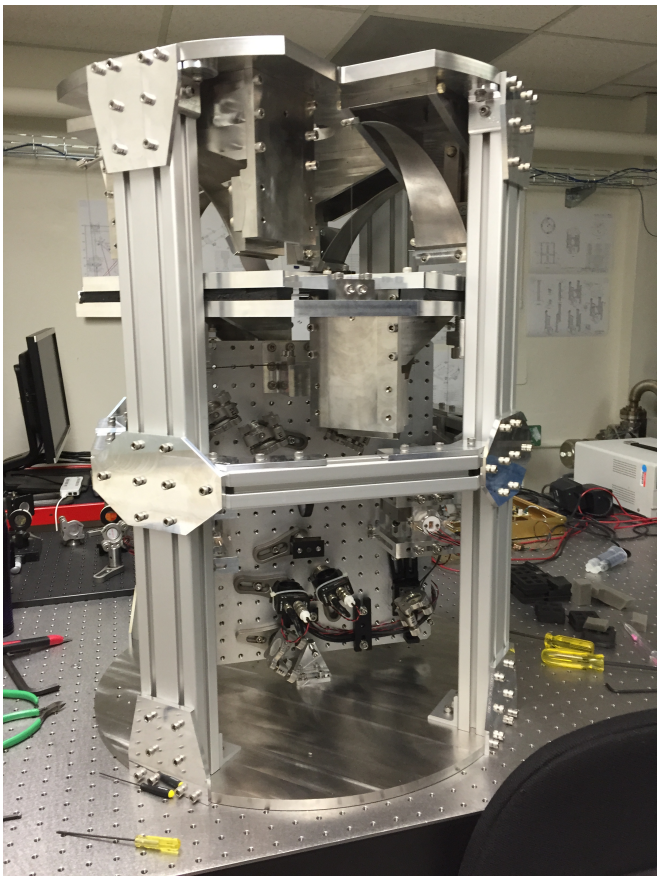

Figure 2: Complete setup

2.2.1 Optical layout

The optical layout schematic in figure 3 below.

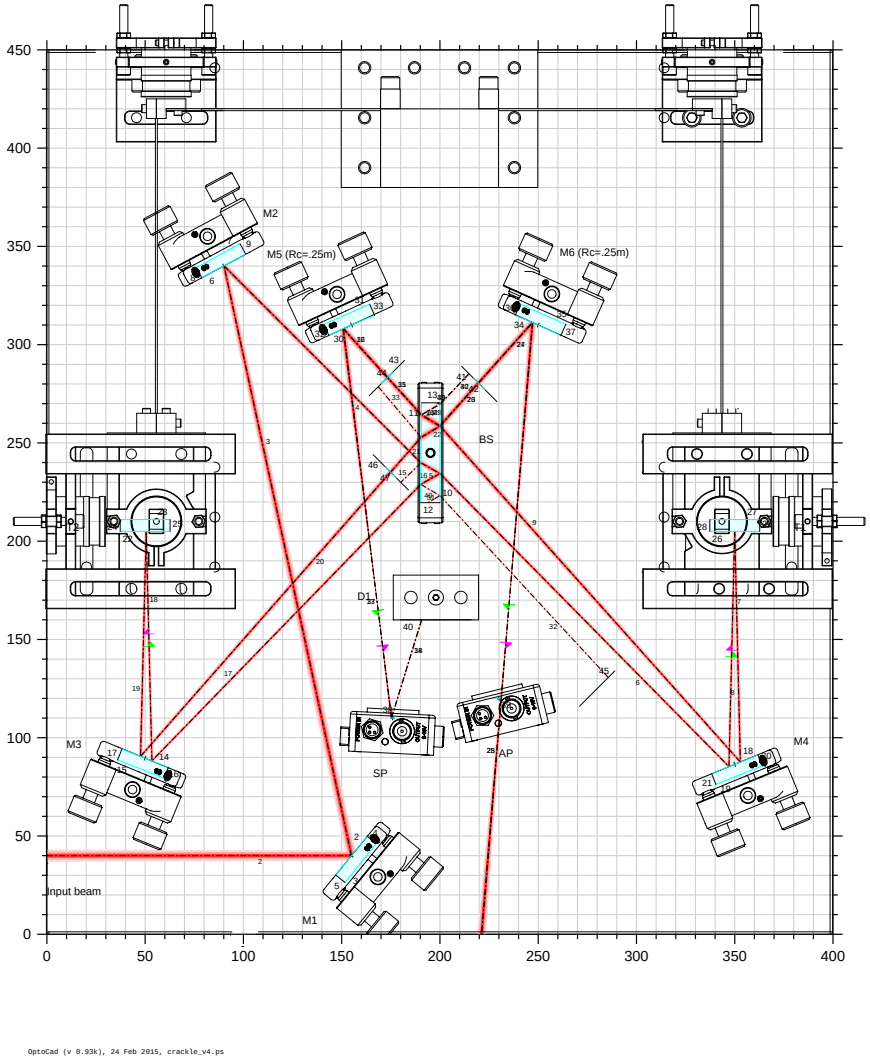

Figure 3: Optical layout

Light from the laser comes in from the bottom left corner through a viewport. Two folding mirrors then redirect the beam to the beam splitter. The two arms of the Michelson interferometer are folded in such a way that the beams impinging on the end mirrors are almost vertical, but tilted enough so that the beams propagating in opposite directions (before and after reflection from the mirror) are separate. The end mirrors of the Michelson arms are horizontal.

2.2.2 Seismic isolation system

Earlier versions of the setup used a stack of two steel plates resting on blocks made of rubber to provide isolation of the Michelson from the ground motion. Ideally, seismic motion of the optical setup wouldn't couple to the Michelson signal because the motion would be common to both mirrors. However, any differential motion of the blades would result in a spurious signal.

Lately, a suspension system has been employed for the breadboard with the Michelson interferometer. A basic control of the breadboard has already been established, and a more detailed modeling of the system and damping in all six d.o.f. is to be implemented.

Figure 4 below shows a simplified scheme of the suspension system. Vertical isolation has been achieved using maraging steel spring blades. A two stage system has been designed. The upper stage is composed of four such blades, each one supporting a wire which are attached to an intermediate stage.

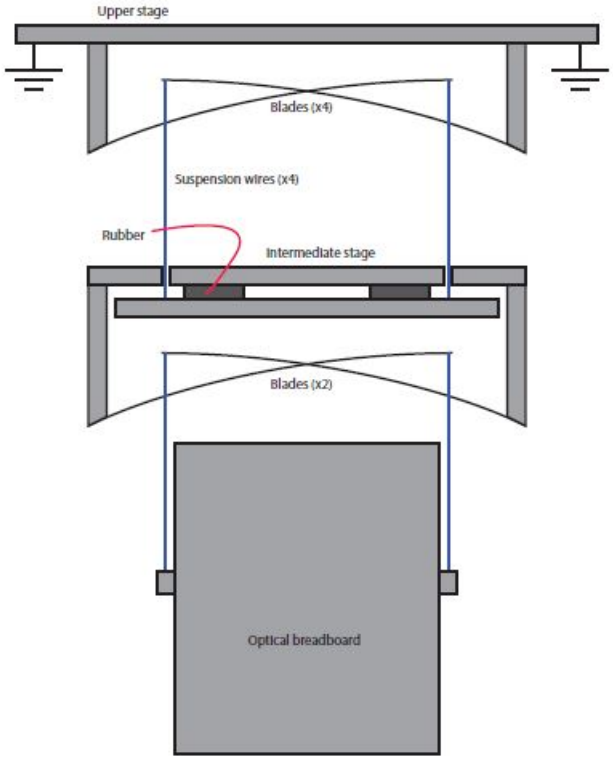

Figure 4: Scheme of the suspension system

3 Progress

The problem statement for my project, to put it in very simple words, is to implement a damping feedback control loop for the suspended optical breadboard. The following subsections are written

in an order so as to build up to the said aim.

3.1 Sensing motion of breadboard using OSEM

This subsection talks about using the suspension OSEM to track the motion of the breadboard in physical degrees of freedom.

3.1.1 Analytical model

Figure 5 shows the mounting scheme of the six OSEMs.

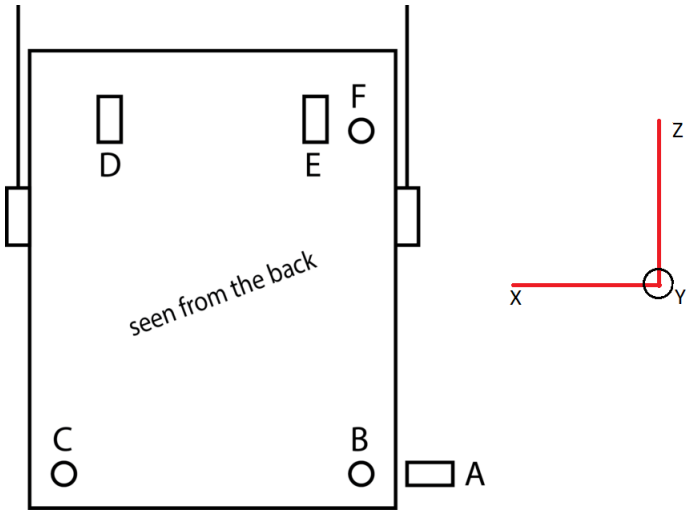

Figure 5: Scheme of OSEMs

It is possible to use the outputs of these shadow sensors to sense motion of the suspended breadboard. Here, I build an analytical model for the same.

I start with the basic relation that gives the velocity $\mathbf{v_p}$ at a point P whose position vector is $\mathbf{r_p}$ on a rigid body whose center of mass (CM) moves with a velocity $\mathbf{v_{cm}}$. The angular velocity is ω. The relation can be written as:

$$\mathbf{v_p} = \mathbf{v_{cm}} + \omega \times \mathbf{r_p} \tag{1}$$

In an infinitesimal time interval, the equation can be rewritten as:

$$\mathbf{s_p} = \mathbf{s_{cm}} + \mathbf{d\theta} \times \mathbf{r_p} \tag{2}$$

where now, $\mathbf{s_p}$ is the infinitesimal displacement vector of the point P, $\mathbf{s_{cm}}$ is the infinitesimal displacement vector of the center of mass and $\mathbf{d\theta}$ represents infinitesimal rotation of the position vector of point P, $\mathbf{r_p}$, about the center of mass.

Equation (2) can be written in the matrix form as:

$$\begin{pmatrix} s_{p,x} \\ s_{p,y} \\ s_{p,z} \end{pmatrix} = \begin{pmatrix} 1 & 0 & 0 & 0 & -r_{p,z} & r_{p,y} \\ 0 & 1 & 0 & r_{p,z} & 0 & -r_{p,x} \\ 0 & 0 & 1 & -r_{p,y} & r_{p,x} & 0 \end{pmatrix} \begin{pmatrix} s_{cm,x} \\ s_{cm,y} \\ s_{cm,z} \\ d\theta_x \\ d\theta_y \\ d\theta_z \end{pmatrix} \tag{3}$$

Here, $s_{p,x}$ corresponds to displacement of point P in the x direction.

Now, in the case of interest here, each of the 6 sensors has one such matrix equation. However, note that by construction, **each OSEM can measure displacement for only motion along its axis**. Coupling this with the fact that each of the six sensors are mounted such that their axis is along one of the principal axes (as can be seen in figure 5), it is clear that **only one of the three linear equations represented in equation (3) becomes relevant**.

Let us see this for an example: sensor A. The equation corresponding to $s_{a,x}$ alone becomes relevant because the axis of sensor A is along the absolute (w.r.t ground) x-axis. Therefore, the exact linear equation governing $s_{a,x}$ can be written down by finding out the values of $r_{a,z}$ and $r_{a,y}$. The same can be repeated for all the 6 sensors to obtain a set of 6 linear equations. Notice that the terms on the left hand side of these equations correspond to displacements along sensor axes, and those on the right hand side to motion of the center of mass and rotation about the absolute (w.r.t. ground) axes: roll, pitch and yaw. The desired matrix transformation equation can, then, be established from these six equations. We will see the exact matrix in the next part.

3.1.2 Constructing the transformation: Sensing matrix

As mentioned above, the sensing transformation matrix can be arrived at using the set of 6 linear equations. The positions of the sensors **w.r.t the CM** fix the constants of the matrix.

1. **Finding coordinates of the center of mass (CM)**
   First, we find out the coordinates of the CM. The origin is as shown in figure 3. The suspension is as shown in figure 4. The axis convention is shown in figure 5.

   The y-coordinate can be simply found to be -27 (in mm) by noticing the position of the suspension wires from the center plane of the breadboard.

   For the x and z coordinates, I have estimated the mass and position of various components of the setup. Table 1 summarizes the same.

Table 1: Calculation of CM coordinates of the setup

Item(s)	**Mass (kg)**	**Absolute (w.r.t. ground) coordinates (in xz plane)**	**Comments**
Optical posts and components	12 x 0.4 = 4.8	(-182.167, 177.75)	0.2kg is the weight of each post, and 0.2kg accounts for the mass of the component placed on it. Figure 2 shows the positions of these posts/components. The coordinates posted here correspond to the CM of the system of posts and components
Suspended block 1	2.2	(-44, 210)	
Suspended block 2	2.2	(-356, 210)	
Fixed block	1.45	(-200, 400)	This is the block to which steel blades are clamped
Breadboard	5.9	(-200, 225)	
Reinforcement 1	1.97	(-20, 225)	Mass calculated from material and dimensions
Reinforcement 2	1.97	(-20, 225)	Mass calculated from material and dimensions

Upon calculation, the center of mass of the system comes out to be: 20.49kg at **(-195, -27, 223)** (in mm).

2. **Calculation of positions of sensors w.r.t CM** The next thing I did was to find out the positions of each of the sensors in the absolute (w.r.t. ground) reference frame, and then find their coordinates in the center of mass frame. Refer to table 2. 'X' means that we don't care about that particular coordinate since it is along the axis of the sensor.

Table 2: Positions of sensors

Sensor	**Absolute (w.r.t. ground) coordinates**	**Coordinates in CM frame**
A	(X, 0, 62.5)	(X, 27, -160.6)
B	(-376, X, 62.5)	(-180.16, X, -160.6)
C	(-24, X, 62.5)	(171.82, X, -160.6)
D	(-84, 25.7, X)	(111.82, 52.7, X)
E	(-316, 25.7, X)	(-120.18, 52.7, X)
F	(-376, X, 397)	(-180.18, X, 173.91)

The matrix transformation equation can then be written as:

$$\begin{pmatrix} s_a \\ s_b \\ s_c \\ s_d \\ s_e \\ s_f \end{pmatrix} = \begin{pmatrix} 1 & 0 & 0 & 0 & 160.6 & 27 \\ 0 & -1 & 0 & 160.6 & 0 & -180.18 \\ 0 & -1 & 0 & 160.6 & 0 & 171.82 \\ 0 & 0 & 1 & -52.7 & 111.82 & 0 \\ 0 & 0 & 1 & -52.7 & -120.18 & 0 \\ 0 & -1 & 0 & -173.91 & 0 & -180.18 \end{pmatrix} \begin{pmatrix} s_{cm,x} \\ s_{cm,y} \\ s_{cm,z} \\ d\theta_x \\ d\theta_y \\ d\theta_z \end{pmatrix} \tag{4}$$

3.2 Reconstruction of breadboard motion in 6D

Having constructed the sensing matrix, the next thing I did was to try it out on some real data. The sensor data was exported to struct files using the ligoDV interface. (The MATLAB ligoDV interface can be used to acquire sensor data, from a specified period of time, from the relevant server. In this report, I will not delve into any technical details of the interface or the settings.)

I wrote a MATLAB script that extracted sensor data arrays in double format from the struct files. Since we are interested in infinitesimal displacements around the equilibrium point, I subtracted from each sensor data array the mean of the data. Then, I inverted the transformation matrix from equation 4 to reconstruct motion in the ground frame. (**Care was taken to convert the constants in the transformation matrix from mm to micron.**)

Figure 6 shows plots of motion in 6 d.o.f.

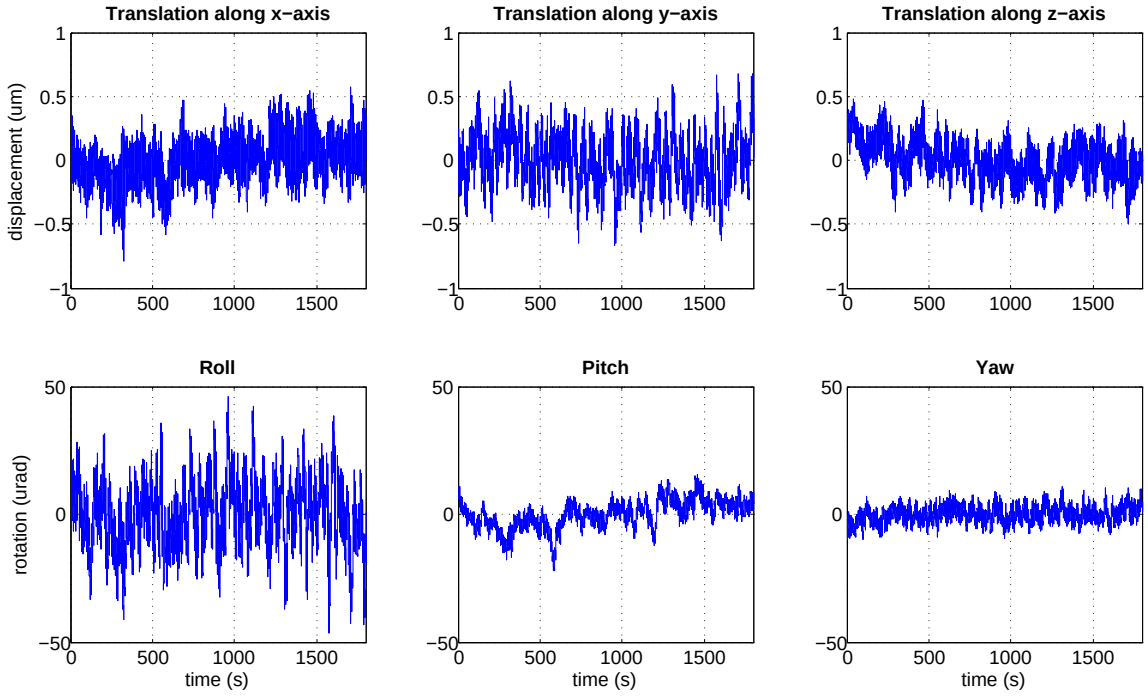

Figure 6: Plot of motion in 6 d.o.f

Notice that the order of magnitude of motion is only a fraction of a micron. These plots cannot really reveal any interesting information. What can be more interesting is the spectra of these motions: one can see the modes and resonance frequencies.

3.3 Spectral analysis

I have used the pwelch function in MATLAB to find the power spectral density (PSD) of the collected motion data. The following points summarize the process.

- `[Pxx,f] = pwelch(data, hanning(nfft), nfft/2, nfft, fs)`

  on MATLAB gives the PSD **Pxx** and the corresponding frequency array **f**
- nfft was chosen to be 1/6th of the total number of points, so as to guarantee about 10 averages through hamming windowing.
- fs represents the sampling frequency, it is equal to 2048Hz.
- The square root of the PSD, amplitude, was used in the plots.

Figure 7 shows the spectra corresponding to motion shown in figure 6.

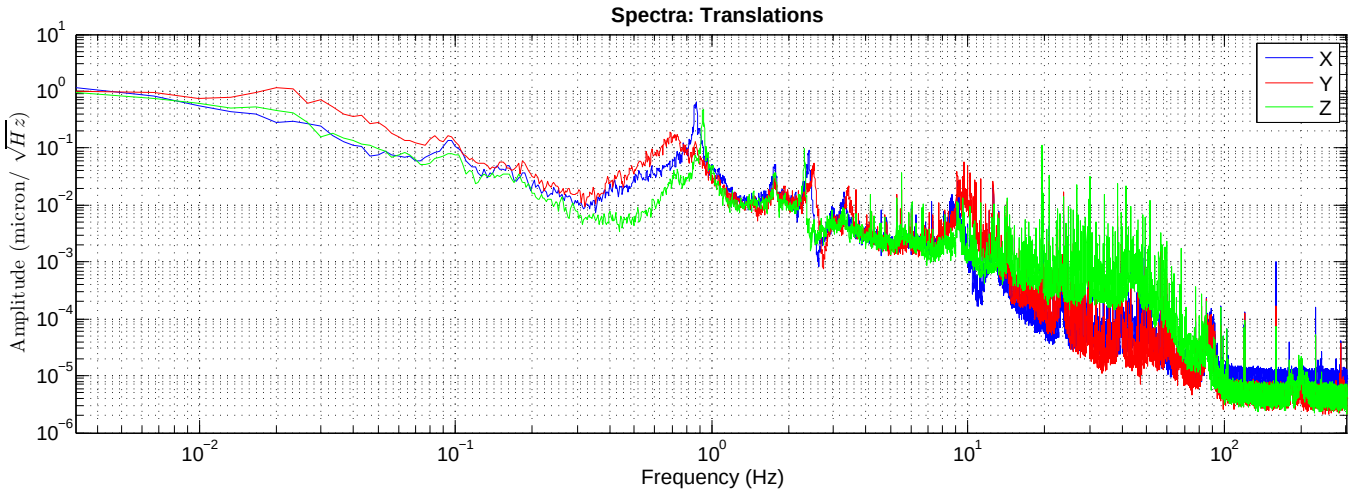

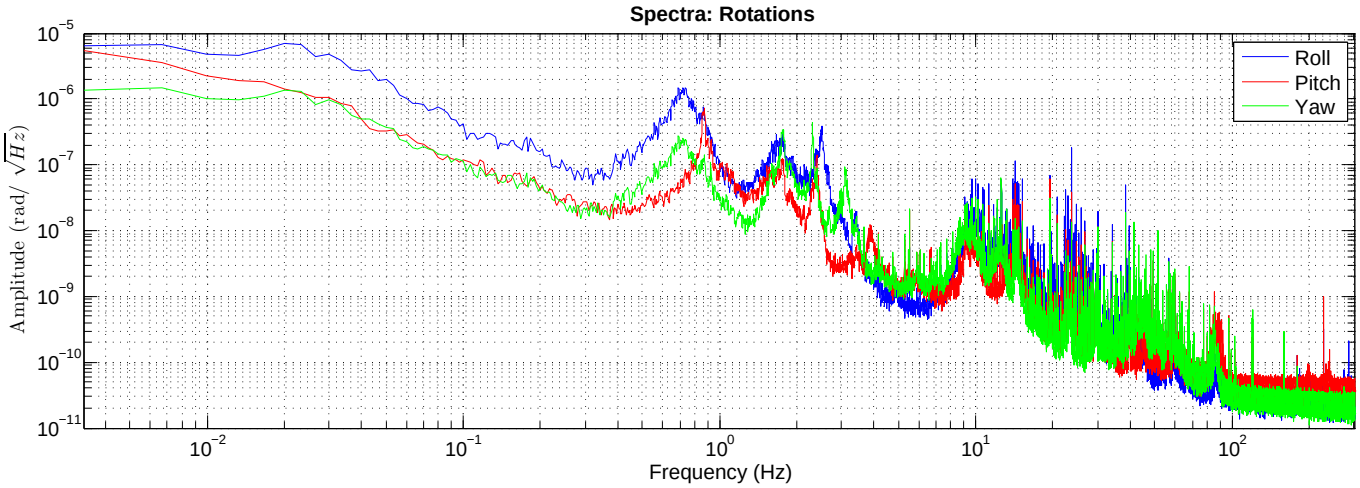

Figure 7: Spectra of motion in 6 d.o.f

From the plots in figure 7, one can infer that:

1. The breadboard is suspended, and the OSEMs are fixed relative to the ground. Most of what is seen in the spectrum is due to motion of the ground (seismic activity); this seems to be concentrated in the $<$10Hz region. **This is what forms the region of interest for us: the aim would be to damp motion at resonant frequencies of the suspension in this range, to achieve better seismic isolation.**

2. All the plots peaks at a particular (common) frequency just below 1Hz – one of the mode frequencies of the system. A few more peaks can be seen for a few frequencies in between 1Hz and 10Hz.

The idea is to damp motion of the breadboard at resonant frequencies. This would require us to have an idea of the mechanical response of the system for damping using OSEM coils at positions A through F. This forms the next part of my work.

3.4 Characterization of mechanical response of the suspension

Six OSEMs, A through F, are mounted at different positions in the cage in which the breadboard is suspended. The scheme has been depicted in figure 5. It is important to understand how OSEMs function in order to get a feel for these measurements.

3.4.1 Detour: A brief about sensing and actuation using OSEM

Optical **S**hadow Sensor and **E**lectro**M**agetic Actuator (OSEM) consists of a shadow sensor part and an electromagnetic actuator part. The former consists of an LED and a photodetector mounted

opposite to each other, as shown in figure 8. Insertion of an object through the hole would block the light from the LED reaching the photodetector, and this change can be used to quantify the extent to which the object has come inside the hole. The actuator part consists of a coil which can generate magnetic field upon driving current through it.

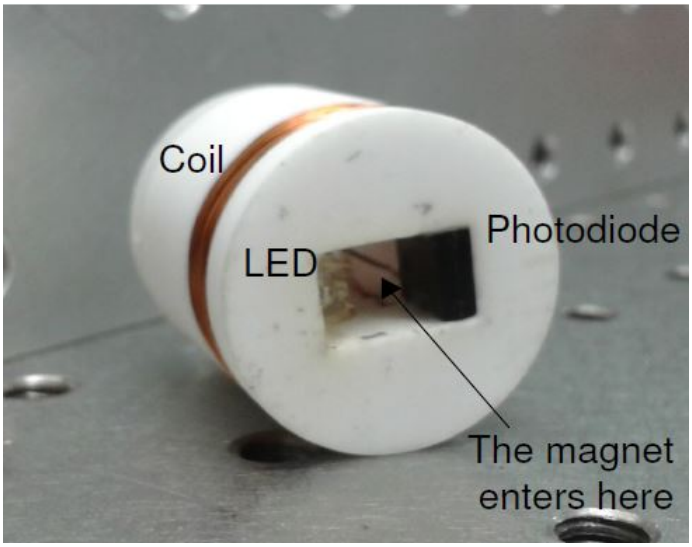

Figure 8: Optical Shadow Sensor and Electromagnetic Actuator

Upon thought, one can easily see that both sensing and actuation can be done by the same unit by simply using a magnetic material for the object whose displacement is to be sensed; and this is precisely what is done: magnets are attached to the points on the breadboard indicated by points A through F. The OSEM modules are mounted outside the suspension, and they are at rest w.r.t the ground.

Then, motion of the magnet can be sensed as usual, and it can even be driven by varying the current through the coil. This is what is used as an actuation for the breadboard.

3.4.2 Measurement of transfer functions

Characterization of the mechanical response of the system consists of exciting one of the coils and recording response in all other sensors or in motion in physical d.o.f. Both are equivalent and are related by the same transformation as the displacements are.

Work is currently underway in this part. So far, I have obtained transfer function data for the case where coil B was excited, among others. I used a sweep sine process for frequencies between 0.5Hz and 15Hz, with an amplitude of 750uN. This gave peak counts (of the coil B output) of about 11,000 at 15Hz. (Whitening and de-whitening filters are active, and so output counts depend on frequency.)

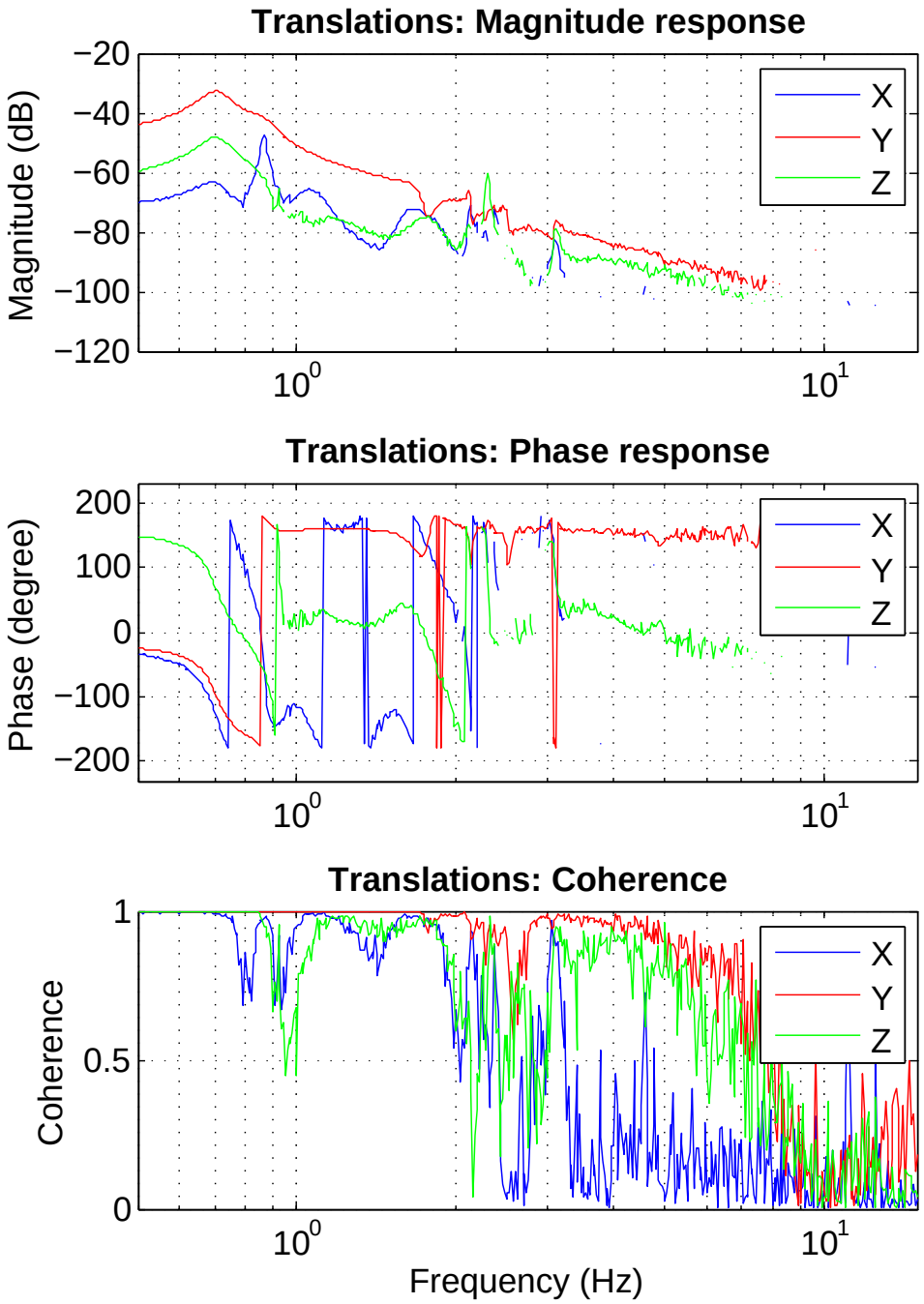

Figure 9: Bode plots for 3 translational d.o.f for the case of coil B excitation

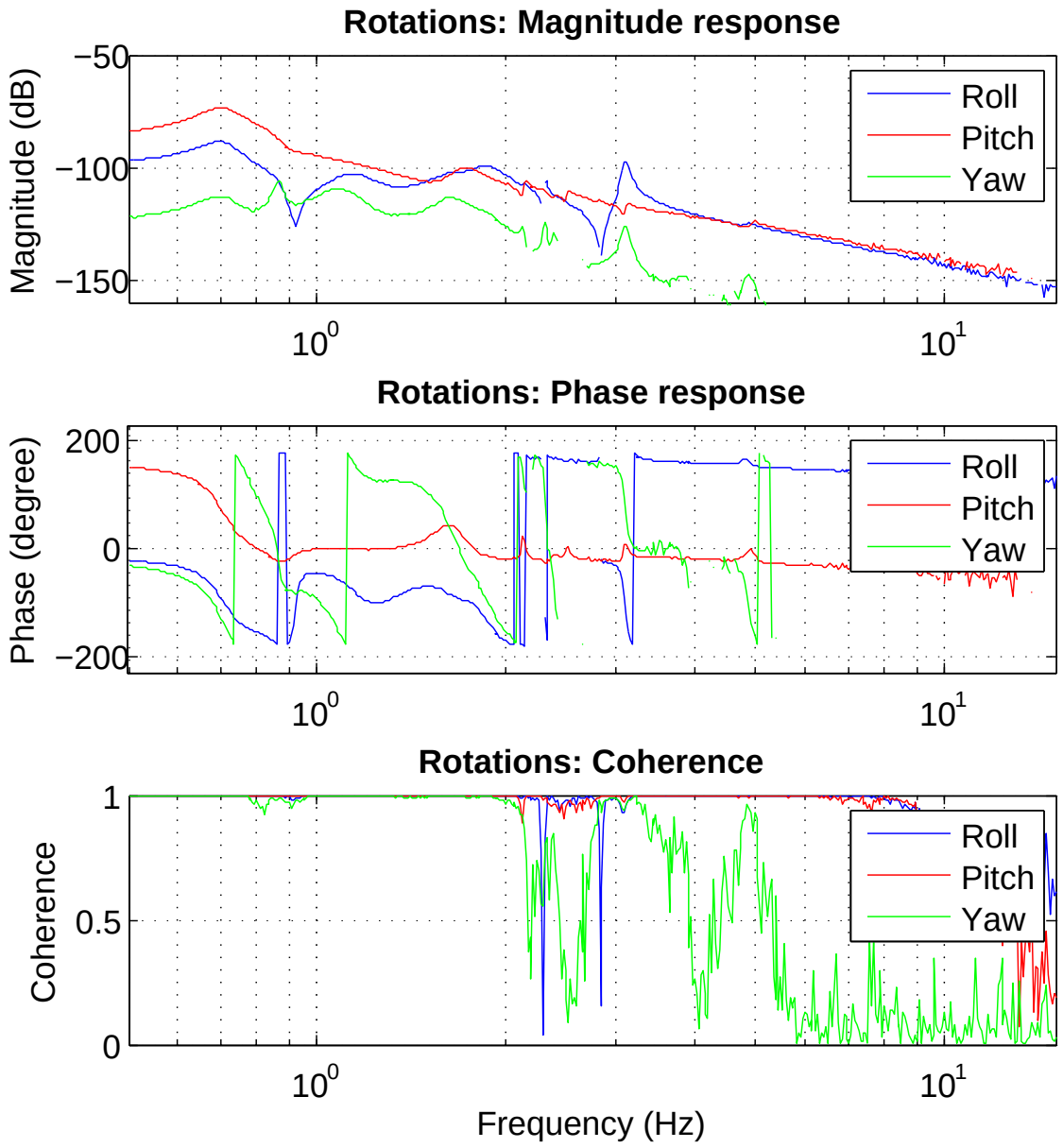

Figure 10: Bode plots for 3 rotational d.o.f for the case of coil B excitation

Figures 9 and 10 show the magnitude, phase and coherence plots (Bode plots) of motion in physical d.o.f. for excitation in coil B. Notice that the peak just below 1Hz still prevails - resonance frequency of the system.

Note that there are quite a few missing points: these plots only consist of points for which the coherence of measurement is above 0.5. A plot of coherence for the collected data is shown in figure 11. One of the immediate aims is to modify the excitation amplitude profile and other parameters to improve coherence.

As mentioned before, work is still underway in this part, and the aim is to collect all the necessary

transfer function data before moving to the next part. After this, transfer function models can be fit to the collected data and poles and zeros of the transfer function can be identified.

4 Up next

The first thing to finish right now would be collecting transfer function data, fit models and find poles and zeros to characterize the system. Then, I will work on modifying the analytical (Mathematica) model that was developed earlier to model the new system, and try to match the analytical transfer function results to the experimentally obtained ones. The setup is going to be re-assembled after the vacuum chamber arrives. I will spend some time on repeating these measurements again, and then move on to implement feedback damping control. Should I find enough time, I could either try and use the blocks and block sensors as inertial sensors, or I could work on the crackle experiment data, depending on the time available. I have summarized these in the following table.

Table 3: Timeline

Week	**Task planned**
1 - 8 June	Characterize the mechanical response of the suspension: finish data acquisition, find poles and zeros of all transfer functions
8 - 15 June	Finish characterization; begin work on analytical model
15 - 22 June	Continue working on analytical model, generate transfer functions, compare with experimentally obtained results
22 - 29 June	Finish work on analytical model and comparisons; Start implementing feedback damping control
21 June - 6 July	Finish implementing control
6 - 20 July	Work on either crackle experiment or on using blocks and block sensors as inertial sensors

References

[1] Xiaoyue Ni, E. Quintero, G. Vajente, ”Proposal for an upgrade of the Crackle experiment”, LIGO-T1400407-v1 (2015)

[2] E. Quintero, E. Gustafson, R. Adhikari, ”Experiment to investigate crackling noise in maraging steel blade springs”, LIGO-T1300465-v2 (2013)